A PERTURBATION ANALYSIS OF NONLINEARITY IN LANDING-GEAR SHIMMY OF A FLEET AIRCRAFT

KOU Minglong[1], ZHANG Jiangang[2], LU Jingming[2], TAN Shengang[2]

[1] AECC CAE, Shanghai 201108, China
[2] AVIC The First Aircraft Institute, Xi'an 710089, China

Abstract

The shimmy damper of a fleet aircraft is hydraulic motor in which more friction and freeplay exists compared to the other forms of shimmy damper, in addition, freeplay of the nose landing gear will increase in later service. A perturbation analysis of nonlinear shimmy in the landing gear is presented. The method is used to obtain general expressions for the limit cycle amplitude and frequency which are functions of ground speed. The analysis shows that stable or unstable limit cycles can exist for taxi speeds above or below a critical value with stability of the limit cycles being determined by the sign of a computed coefficient. The solution method is applied to a dual wheel nonlinear shimmy model. The analysis shows that when only Coulomb friction is present, an unstable limit cycle exist beyond the critical velocity; When only freeplay is present, a stable limit cycle exists below the critical velocity. Both freeplay and Coulomb friction is present, a stable limit cycle exists below the critical velocity; Pilot should do his best to reduce disturbance when landing to avoid shimmy and to decrease taxi speed below the critical velocity; If possible, increasing the critical velocity by strengthening twist stiffness of nose landing gear of the fleet aircraft.

Keywords: perturbation analysis; shimmy; fleet aircraft; freeplay; Coulomb friction

1. Introduction

The prevention of landing gear shimmy continues to be important in the design of aircraft. Typically, both linear and nonlinear shimmy analysis are conducted and by appropriate changes in the geometric, damping, and structural parameters, a shimmy free configuration is sought. However, linear models will fail to predict accurately the behavior of the inherently nonlinear landing gear system and explain why the system is stable when the disturbance is smaller than some value and vice versa. The damper of one fleet aircraft is driven by the gear between hydraulic motor and collar and there are three pairs gear joints in hydraulic rotor besides the presence of Coulomb friction between the oleo struts and freeplay in the torque links, so the nonlinearity of freeplay and coulomb is more stronger than other aircrafts. Besides, analytical solutions to nonlinear shimmy models have appeared in the published literature in only a few cases. This paper establishes a nonlinear shimmy model of a fleet aircraft for engineering application and find the analytical solutions at a given equilibrium point using a perturbation analysis, the method of multiple-time-scales is applied to general autonomous self-excited systems to obtain expressions for the limit cycle amplitude and frequency, and associated stability criteria.

2. Theory of Perturbation Analysis of Shimmy

The nonlinear shimmy models considering freeplay and Coulomb friction is presented as follows:

$$\boldsymbol{M}\ddot{\boldsymbol{q}} + \boldsymbol{K}\boldsymbol{q} = \widehat{\boldsymbol{F}}_{\boldsymbol{j}} sgn(q_j) + \widehat{\boldsymbol{F}}_{\boldsymbol{k}} sgn(\hat{F}_{fp}, q_k) \tag{1}$$

$$\mathrm{sgn}(q_j) = \begin{cases} 1, \mathrm{q}_j > 0 \\ 0, \mathrm{q}_j = 0 \\ -1, \mathrm{q}_j < 0 \end{cases} \tag{2}$$

$$\hat{F}_{fp} = \begin{cases} -k_\theta \theta_{fp}, q_k > +\theta_{fp} \\ -k_\theta q_k, |q_k| \le +\theta_{fp} \\ -k_\theta \theta_{fp}, q_k < -\theta_{fp} \end{cases} \tag{3}$$

M and ***K***(V) are matrices for inertia and viscous damping, and stiffness, respectively; ***q*** is state variable; $\hat{\boldsymbol{F}}_j\, sgn(q_j)$ is the Coulomb friction in steering shimmy system of nose landing gear; $\hat{\boldsymbol{F}}_k(\hat{F}_{fp}, q_k)$ is the torque freeplay in steering shimmy system of nose landing gear. the torque of the steering system of the nose landing gear is given by:

$$F_{fp} = k_\theta q_k + \hat{F}_{fp} \tag{4}$$

Where k_θ is the torque stiffness of nose landing gear, V is the velocity of aircraft.

There is a critical velocity V_0 for linear system ($\hat{\boldsymbol{F}}_j = \hat{\boldsymbol{F}}_k = 0$). When $V < V_0$, the linear system is stable; $V > V_0$, the linear system is unstable; $V = V_0$, there is an pure imaginary root in eigenvalues and all other eigenvalues have real parts. Then, the equation (1) can be solved about the equilibrium point $\boldsymbol{q_e} = \boldsymbol{0}$ with perturbation analysis.

Assume that V can be expanded as a power series in a small parameter ε about the critical point V_0.

$$V = V_0 + \varepsilon V_1 + \varepsilon^2 V_2 + O(\varepsilon^3) \tag{5}$$

Where, coefficients V_i are constants, ε is perturbation parameter.

Stiffness matrics $\boldsymbol{K}(V)$ can be expanded as:

$$\boldsymbol{K}(V) = \boldsymbol{K}^{(0)}(V_0) + \varepsilon \boldsymbol{K}^{(1)}(V_1) + O(\varepsilon^2) \tag{6}$$

Rescale the nonlinear terms by a factor ε:

$$\hat{\boldsymbol{F}}_j = \varepsilon \boldsymbol{F}_j \tag{7}$$

$$\hat{\boldsymbol{F}}_k = \varepsilon \boldsymbol{F}_k \tag{8}$$

Then, equation (1) becomes:

$$\boldsymbol{M}\dot{\boldsymbol{q}} + \boldsymbol{K}\boldsymbol{q} = \varepsilon[\boldsymbol{F_j}\,\mathrm{sgn}(q_j) - \boldsymbol{F_k}] \tag{9}$$

Using the method of multiple time scales, the dependent variable q can be expanded as:

$$\boldsymbol{q} = \sum_{m=0}^{M} \varepsilon^m \boldsymbol{q}_m \tag{10}$$

Define multiple time scales such that

$$\tau_m = \varepsilon^m \tau, \qquad m = 0,1,2... \tag{11}$$

Then,

$$\frac{d}{d\tau} = \sum_{m=0}^{M} \varepsilon^m \frac{\partial}{\partial \tau_m} + O(\varepsilon^{M+1}) \tag{12}$$

$$\frac{d\boldsymbol{q}}{d\tau} = \frac{\partial \boldsymbol{q}_0}{\partial \tau_0} + \varepsilon[\frac{\partial \boldsymbol{q}_0}{\partial \tau_1} + \frac{\partial \boldsymbol{q}_1}{\partial \tau_0}] + \varepsilon^2[\frac{\partial \boldsymbol{q}_2}{\partial \tau_0} + \frac{\partial \boldsymbol{q}_1}{\partial \tau_1} + \frac{\partial \boldsymbol{q}_0}{\partial \tau_2}] + O(\varepsilon^3) \tag{13}$$

Substitution of equations (5)-(6) and (10)-(13) into equation (9), gives the following sets of equations to $O(\epsilon^2)$.

2.1 ϵ^0 Order System

$$\boldsymbol{L}\boldsymbol{q_0} = \boldsymbol{0} \tag{14}$$

$$L = M\frac{\partial}{\partial\tau_0} + K^{(0)} \tag{15}$$

The ϵ^0 order system in equation (14) is the set of linear shimmy equations for small perturbations about the equilibrium point $\boldsymbol{q_e} = \boldsymbol{0}$. The harmonic solution to equation (14) for $\boldsymbol{q_0}$ is

$$\boldsymbol{q}_0 = A\boldsymbol{u}e^{i\psi} + A\boldsymbol{u}^* e^{-i\psi} = 2A\,\mathrm{Re}\,al[\boldsymbol{u}e^{i\psi}] \tag{16}$$

$$\psi = \omega_0\tau_0 + \phi(\tau_1,\tau_2,...) \tag{17}$$

$$A = A(\tau_1,\tau_2,...) \tag{18}$$

Substitution of equations (17) and (18) into equation (16) gives

$$\boldsymbol{L}_0\boldsymbol{u} = 0 \tag{19}$$

$$\boldsymbol{L}_0 = i\omega_0\boldsymbol{M} + \boldsymbol{K}^{(0)} \tag{20}$$

Equations (20) possesses nontrivial solutions if and only if

$$\det \boldsymbol{L_0} = 0 \tag{21}$$

Equations (21) determines the eigenvalue ω_0, and hence the according eigenvector $\mathbf{u}$.

2.2 ϵ^1 Order System

$$\boldsymbol{Lq_1} = \boldsymbol{-K^{(1)}q_0} - \boldsymbol{M}\frac{\partial q_0}{\partial\tau_1} + \boldsymbol{F}_j(V_0,q_0)\,\mathrm{sgn}(q_{j0}) + \boldsymbol{F}_k(V_0,q_0) \tag{22}$$

Expand the nonlinear terms due to Coulomb friction and structural freeplay which appear on the right hand side of (22) in complex Fourier series with

$$\boldsymbol{f}_j^{(n)} = \frac{1}{2\pi}\int_0^{2\pi}\boldsymbol{F}_j\,\mathrm{sgn}(q_{j0})e^{-in\psi}d\psi \tag{23}$$

$$\boldsymbol{f}_k^{(n)} = \frac{1}{2\pi}\int_0^{2\pi}F_k e^{-in\psi}d\psi \tag{24}$$

For $-\infty \le n \le \infty$, and where

$$q_{j0} = 2A\,\mathrm{Re}\,al[u_j e^{i\psi}] \tag{25}$$

Substitute $\boldsymbol{q_0}$ from equation (16) into equations (22), (23), and (24) to obtain an equation for $\boldsymbol{q_1}$.

$$\begin{aligned}\boldsymbol{Lq_1} = &\sum_{-\infty<n<+\infty}^{n\neq\pm1}[\boldsymbol{f}_j^{(n)}(A) + \boldsymbol{f}_k^{(n)}(A)]e^{in\psi} + \\ &[\boldsymbol{f}_j^{(+1)}(A) + \boldsymbol{f}_k^{(+1)}(A) - \boldsymbol{K}^{(1)}\boldsymbol{u}A]e^{+i\psi} - \\ &(\frac{\partial A}{\partial\tau_1} + iA\frac{\partial\psi}{\partial\tau_1})\boldsymbol{Mu}e^{+i\psi} + \\ &[\boldsymbol{f}_j^{(-1)}(A) + \boldsymbol{f}_k^{(-1)}(A) - \boldsymbol{K}^{(1)}\boldsymbol{u}A]e^{-i\psi} - \\ &(\frac{\partial A}{\partial\tau_1} - iA\frac{\partial\psi}{\partial\tau_1})\boldsymbol{Mu}^*e^{-i\psi}\end{aligned} \tag{26}$$

The terms on the right hand side of equation (26) which multiply $e^{i\psi}$ and $e^{-i\psi}$ are secular and lead to spurious resonance which can be suppressed by requiring that

$$\boldsymbol{v^T}[-\boldsymbol{f}_y^{(+1)}(A) - \boldsymbol{f}_z^{(+1)}(A) + \boldsymbol{K}^{(1)}\boldsymbol{u}A] + \boldsymbol{v^T}(\frac{\partial A}{\partial\tau_1} + iA\frac{\partial\psi}{\partial\tau_1})\boldsymbol{Mu} = 0 \tag{27}$$

Or

$$\beta A + \gamma + \delta + (\frac{\partial A}{\partial\tau_1} + iA\frac{\partial\psi}{\partial\tau_1}) = 0 \tag{28}$$

where

$$\sigma = \boldsymbol{v^T Mu} \tag{29}$$

$$\mu = \mathbf{v}^T \boldsymbol{K}^{(1)} \mathbf{u} / \sigma \tag{30}$$

$$\gamma = -\mathbf{v}^T \boldsymbol{f}_y^{(+1)} \mathbf{u} / \sigma \tag{31}$$

$$\delta = -\mathbf{v}^T \boldsymbol{f}_k^{(+1)} \mathbf{u} / \sigma \tag{32}$$

v is the left eigenvector associated with

$$\mathbf{v}^T \boldsymbol{L}_0 = \boldsymbol{0}^T \tag{33}$$

By equating the real and imaginary parts in equation (28) to zero individually, partial different equations are obtained for the amplitude A and phase ψ

$$\mu_R A + \gamma_R + \delta_R + \frac{\partial A}{\partial \tau_1} = 0 \tag{34}$$

$$(\frac{\partial \psi}{\partial \tau_1} + \mu_I) A + \gamma_I + \delta_I = 0 \tag{35}$$

Gordon[18] compared the first order system solution with direct numeric integration solution, and found that the compliance is good. We also take the first order system in this paper.

2.3 Limit Cycle Solution

For stationary periodic motion, $\partial A / \partial \tau_1 = 0$, and from equation (34) the limit cycle solution is obtained.

$$G(A) = \mu_R A + \gamma_R + \delta_R = 0 \tag{36}$$

The combination of equations (10), (16), (17) and (18), take $\varepsilon = (V - V_0)/V_1$, we get

$$\boldsymbol{q} = 2\left|(\gamma_R + \delta_R) / \mu_R\right| \mathrm{Re}\, al[\boldsymbol{u} e^{iw\tau_0}] + O(\varepsilon) \tag{37}$$

the phase ψ and shimmy frequency ω can be determined through equation (17) and equation (35).

$$\psi = \omega_0 \tau_0 - \varepsilon \left[\mu_I + \frac{(\gamma_I + \delta_I)}{A_{LC}} \right] \tau_0 \tag{38}$$

$$\omega = \omega_0 - \varepsilon \left[\mu_I + \frac{(\gamma_I + \delta_I)}{A_{LC}} \right] \tag{39}$$

The amplitude of limit cycle $2A = 2A_{LC}$ is determined by equation (36), take $\varepsilon = 1$

2.4 Nonlinear Stability Analysis

The partial differential equation (34) is solved as

$$A = K(\tau_2, \tau_3, \ldots) e^{-\mu_R \tau_1} - ((\gamma_R + \delta_R) / \mu_R) \tag{40}$$

When $A(\tau_1 = 0) = A_0$, $K = A_0 + (\gamma_R + \delta_R) / \mu_R$, then

$$A = (A_0 + (\gamma_R + \delta_R) / \mu_R) e^{-\mu_R \tau_1} - ((\gamma_R + \delta_R) / \mu_R) \tag{41}$$

Stability of the limit cycle is determined by evaluation of $G'(A) = dG/dA$. The limit cycle is stable for $G'(A_{LC}) > 0$ and unstable for $G'(A_{LC}) < 0$.

3. Shimmy Analysis of a Fleet Aircraft

3.1 Shimmy model

It is a dual wheel strut nose landing gear having no inclined angle, the parameters and variables used for shimmy analysis is in table 1, analysis software is Matlab_R2012a.

Table 1 Parameters and variables for shimmy analysis

Parameter	Description	Value
C_{cf}	Half Coulomb friction coefficient	5N.m
θ_{fp}	Effective torsional freeplay	0.001rad
I_z	Moment of inertia of gear	7.5kg.m^2
k_θ	Half torsional stiffness of gear	3×10^4 N.m/rad
a	Lateral stiffness of tire	1.8×10^{6}N/m
b	Torsional stiffness of tire	2.9×10^{6}N.m/rad
B	Half wheel distance	0.21m
C	Longitudinal stiffness of tire	0.16m
t	Mechanical caster	0.3m
d	Tire diameter	0.51
W	Tire width	0.14
α	Lateral roll coefficient of tire	139.7
β	Torsional roll coefficient of tire	35.6
θ	Yaw angle	variable
$\dot{\theta}$	Velocity of yaw angle	variable
λ	Lateral displacement	variable
ϕ	Torsional displacement	variable
V	Taxing velocity	variable
F_{fp}	Effective moment in torque link	variable
F_{cf}	Coulomb moment between oleos	variable

First, build the fourth linear shimmy equations (42) according to the reference[1]. Then, solve the equations (42) to get the critical velocity under various velocity and running load based on the Hurwitz theorem, and get the required damping value $h = 210N.m.s/rad$ based on the convergency criterion[21].

$$\begin{cases} \frac{1}{2}I_z\ddot{\theta}+\frac{1}{2}h\dot{\theta}+CB^2\theta-at\lambda-b\phi=0 \\ t\dot{\theta}+\dot{\lambda}+V\theta+V\phi=0 \\ \dot{\theta}+\dot{\phi}-V\alpha\lambda+V\beta\phi=0 \\ \dot{\theta}-\dot{\theta}=0 \end{cases} \tag{42}$$

Build the fourth nonlinear shimmy equations (43) considering Coulomb friction and freeplay, and the equations (43) is solved by the perturbation analysis mentioned at chapter 2.

$$\begin{cases} \frac{1}{2}I_z\ddot{\theta}+\frac{1}{2}h\dot{\theta}+CB^2\theta-at\lambda-b\phi=-F_{fp}-F_{cf} \\ t\dot{\theta}+\dot{\lambda}+V\theta+V\phi=0 \\ \dot{\theta}+\dot{\phi}-V\alpha\lambda+V\beta\phi=0 \\ \dot{\theta}-\dot{\theta}=0 \end{cases} \tag{43}$$

Where,

$$F_{fp}=k_\theta\theta+\hat{F}_{fp} \tag{44}$$

$$\hat{F}_{fp} = \begin{cases} -k_\theta \theta_{fp}, \theta > +\theta_{fp} \\ -k_\theta \theta, \quad |\theta| \le +\theta_{fp} \\ +k_\theta \theta_{fp}, \theta < -\theta_{fp} \end{cases} \tag{45}$$

$$F_{cf} = C_{cf}\,\mathrm{sgn}(\dot{\theta}) \tag{46}$$

$$\mathrm{sgn}(\dot{\theta}) = \begin{cases} +1, \dot{\theta} > 0 \\ 0, \dot{\theta} = 0 \\ -1, \dot{\theta} < 0 \end{cases} \tag{47}$$

Rewrite equation (43) as matrix form

$$\boldsymbol{M}\dot{\boldsymbol{q}} + \boldsymbol{K}\boldsymbol{q} = \hat{\boldsymbol{F}}_{cf}\,\mathrm{sgn}(\dot{\theta}) + \hat{\boldsymbol{F}}_{fp} \tag{48}$$

$$\boldsymbol{q} = \{q_1, q_2, q_3, q_4\}^T = \{\dot{\theta}, \theta, \lambda, \phi\}^T \tag{49}$$

$$\boldsymbol{M} = \begin{bmatrix} \frac{1}{2}I_z & \frac{1}{2}h & 0 & 0 \\ 0 & t & 1 & 0 \\ 0 & 1 & 0 & 1 \\ 0 & 1 & 0 & 0 \end{bmatrix} \tag{50}$$

$$\boldsymbol{K} = \begin{bmatrix} 0 & CB^2 + k_\theta & -at & -b \\ 0 & V & 0 & V \\ 0 & 0 & -V\alpha & V\beta \\ -1 & 0 & 0 & 0 \end{bmatrix} \tag{51}$$

$$\hat{\boldsymbol{F}}_{fp} = -\begin{bmatrix} \hat{F}_{fp} \\ 0 \\ 0 \\ 0 \end{bmatrix} \tag{52}$$

$$\hat{\boldsymbol{F}}_{cf} = -\begin{bmatrix} C_{cf} \\ 0 \\ 0 \\ 0 \end{bmatrix} \tag{53}$$

According to equation (6)

$$\boldsymbol{K}^{(0)} = \begin{bmatrix} 0 & CB^2 + k_\theta & -at & -b \\ 0 & V_0 & 0 & V_0 \\ 0 & 0 & -V_0\alpha & V_0\beta \\ -1 & 0 & 0 & 0 \end{bmatrix} \tag{54}$$

$$\boldsymbol{K}^{(1)} = \begin{bmatrix} 0 & 0 & 0 & 0 \\ 0 & V_1 & 0 & V_1 \\ 0 & 0 & -V_1\alpha & V_1\beta \\ 0 & 0 & 0 & 0 \end{bmatrix} \tag{55}$$

For linear system, according to equation (21), separate the real part and imaginary part and make them equal zero, we can get the critical velocity of shimmy $V_0 = 16.469 m/s$, the critical circle frequency of shimmy $\omega_0 = 215.56 rad/s$. And the critical velocity and critical frequency increase with increasing of torsional stiffness, for example, when $k_\theta = 5.0 \times 10^4 N.m/rad$, $V_0 = 19.46 m/s$, $\omega_0 = 243.04 rad/s$.

3.2 Coulomb Friction only

Normalize $\boldsymbol{u}$ and make $\theta = q_{20} = 2A\cos\psi$, left eigenvector and right eigenvector can be obtained by equation (19) and equation (33).

$$\boldsymbol{u}=\begin{bmatrix} i\omega_0 \\ 1 \\ \dfrac{\omega_0{}^2 t - i\omega_0 t V_0 \beta - \beta V_0{}^2}{V_0{}^2\alpha - \omega_0{}^2 + i\omega_0 V_0 \beta} \\ \dfrac{\omega_0{}^2 - i\omega_0 t V_0 \alpha - \alpha V_0{}^2}{V_0{}^2\alpha - \omega_0{}^2 + i\omega_0 V_0 \beta} \end{bmatrix} = \begin{bmatrix} 215.5686i \\ 1 \\ -0.0765+0.0522i \\ -0.3169-0.0463i \end{bmatrix} \tag{56}$$

$$\boldsymbol{v}=\begin{bmatrix} 1 \\ \dfrac{at(i\omega_0+V_0\beta)+V_0\alpha b}{V_0{}^2\alpha - \omega_0{}^2 + i\omega_0 V_0 \beta} \\ \dfrac{i\omega_0 b - atV_0}{V_0{}^2\alpha - \omega_0{}^2 + i\omega_0 V_0 \beta} \\ i\dfrac{1}{2}\omega_0 I_z \end{bmatrix} = \begin{bmatrix} 1 \\ 59.5706-267.9573i \\ 5.2804+5.5801i \\ 343.1796i \end{bmatrix} \tag{57}$$

$\boldsymbol{f}_y^{(+1)}$ can be got by equation (23) using piecewise integration.

$$\boldsymbol{f}_y^{(+1)} = \begin{bmatrix} -3.1831i \\ 0 \\ 0 \\ 0 \end{bmatrix} \tag{58}$$

σ, μ and γ can be obtained by equation (29), equation (30) and equation (31) respectively for every single velocity.

For $V < V_0$, $\mu_R > 0$. Initial value $A_0 \le \left|\frac{\gamma_R}{\mu_R}\right|$ or $A_0 > \left|\frac{\gamma_R}{\mu_R}\right|$, when $V > V_0$, $A \to 0$, according to equation (41), the system is stable.

For $V > V_0$, $\mu_R > 0$. Initial value $A_0 \le \left|\frac{\gamma_R}{\mu_R}\right|$, when $\tau_1 \to \infty$, $A \to 0$; Initial value $A_0 > \left|\frac{\gamma_R}{\mu_R}\right|$, when $\tau_1 \to \infty$, $A \to \infty$. There is unstable limit cycle, in general, the system is unstable. The stability of the limit cycle can also be determined by sign of $G'(A_{LC})$.

Figure 1 is a limit cycle of $V = 36\mathrm{m/s}$, the amplitude of the limit cycle is $2A_{LC} =$ 0.001344. limit cycle is a continuous vibration of which the amplitude is constant; Figure 2 is the amplitude response of A when $A_0 = 0.0001$, which means A is stable when $A_0 < A_{LC}$; Figure 3 is the amplitude response of A when $A_0 = 0.01$, which means A is unstable when $A_0 > A_{LC}$; Figure 4 is the relationship of A and V, when $V < V_0$, the system is stable, and when $V \ge V_0$, the system is unstable and the amplitude of limit cycle is decreasing with V being bigger than V_0, and $G'(A_{LC}) = -6.8415$.Figure 5 is the relationship of limit cycle amplitude and velocity, the unstable area is decreasing with increasing of Coulomb. when $V < V_0$, the system is stable; when $V > V_0$, the system is unstable if the initial disturbance is bigger than limit cycle amplitude.

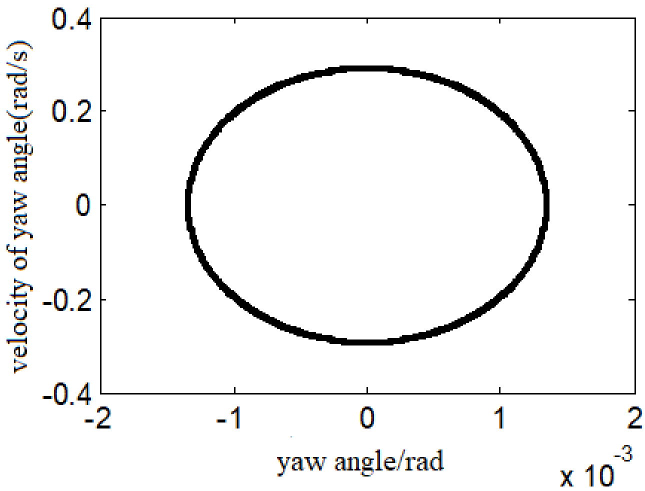

Fig.1 Limit cycle for only Coulomb($C_{cf} = 5N.m, \theta_{fp} = 0$)

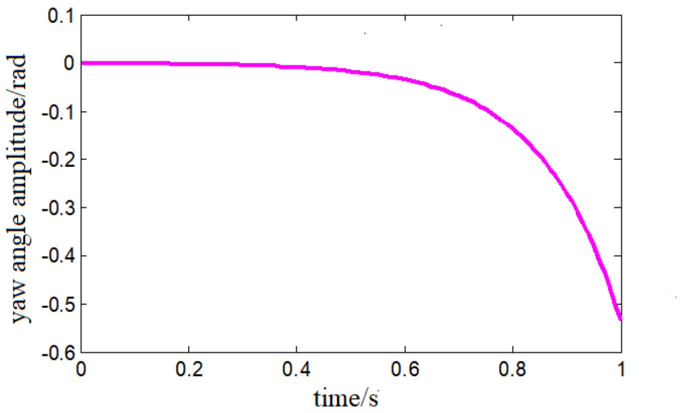

Fig.2 Response of yaw angle for only Coulomb($C_{cf} = 5N.m, \theta_{fp} = 0, A_0 = 0.0001rad$)

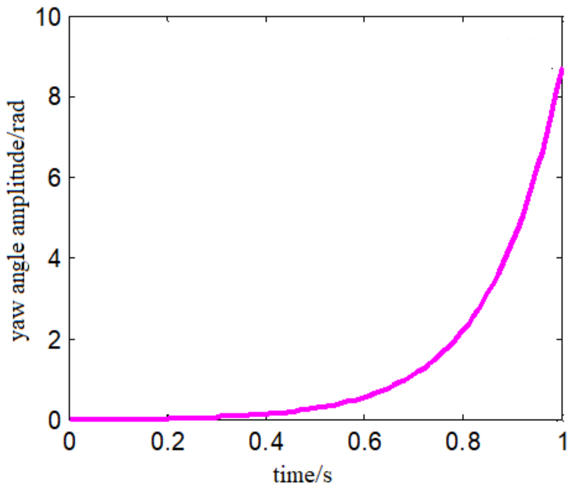

Fig.3 Response of yaw angle for only Coulomb($C_{cf} = 5N.m, \theta_{fp} = 0, A_0 = 0.01rad$)

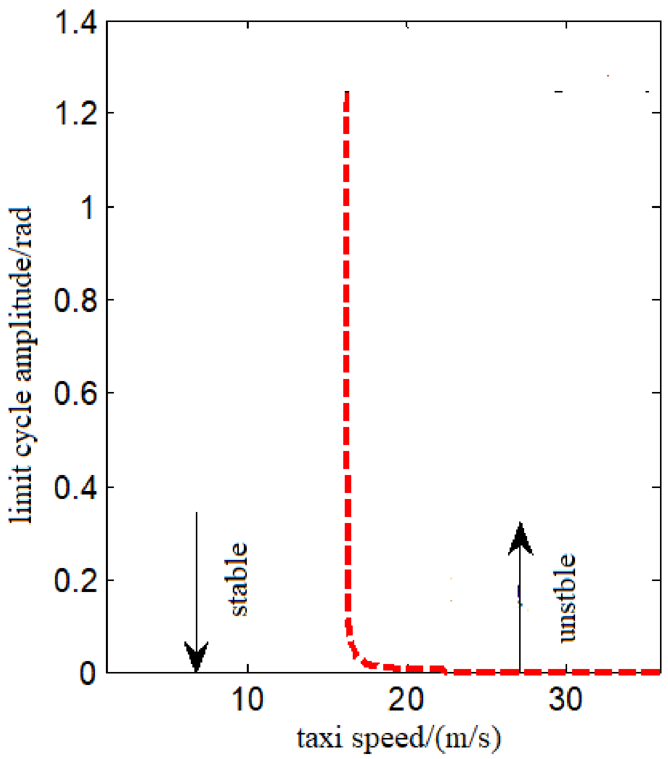

Fig.4 Limit Cycle Amplitude vs Taxi Speed($C_{cf} = 5N.m, \theta_{fp} = 0$)

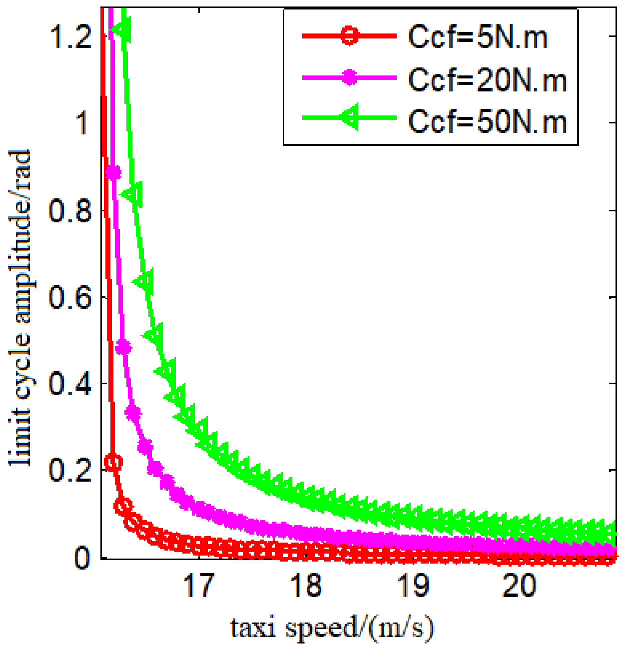

Fig.5 Limit Cycle Amplitude for different Coulomb vs Taxi Speed

3.3 Freeplay only

Normalize $\boldsymbol{u}$ and make $\theta = q_{20} = 2A\sin\psi$, left eigenvector and right eigenvector can be obtained by equation (19) and equation (33).

$$\boldsymbol{u} = \begin{bmatrix} \omega_0 \\ -i \\ \dfrac{-i(\omega_0{}^2 t - i\omega_0 t V_0\beta - \beta V_0{}^2)}{V_0{}^2\alpha - \omega_0{}^2 + i\omega_0 V_0\beta} \\ \dfrac{-i(\omega_0{}^2 - i\omega_0 t V_0\alpha - \alpha V_0{}^2)}{V_0{}^2\alpha - \omega_0{}^2 + i\omega_0 V_0\beta} \end{bmatrix} = \begin{bmatrix} 215.5686 \\ -i \\ 0.0522 + 0.0765i \\ -0.0463 + 0.3169i \end{bmatrix} \tag{59}$$

$$\boldsymbol{v} = \begin{bmatrix} 1 \\ \dfrac{at(i\omega_0 + V_0\beta) + V_0\alpha b}{V_0{}^2\alpha - \omega_0{}^2 + i\omega_0 V_0\beta} \\ \dfrac{i\omega_0 b - atV_0}{V_0{}^2\alpha - \omega_0{}^2 + i\omega_0 V_0\beta} \\ i\dfrac{1}{2}\omega_0 I_z \end{bmatrix} = \begin{bmatrix} 1 \\ 59.5706 - 267.9573i \\ 5.2804 + 5.5801i \\ 343.1796i \end{bmatrix} \tag{60}$$

$\boldsymbol{f}_y^{(+1)}$ can be got by equation (24) using piecewise integration.

$$\boldsymbol{f}_k^{(+1)} = \begin{bmatrix} -19.0981i \\ 0 \\ 0 \\ 0 \end{bmatrix} \tag{61}$$

σ, μ and γ can be obtained by equation (29), equation (30) and equation (31) respectively for every single velocity.

For $V > V_0$, the system is unstable, and we focus on $V < V_0$.Figure 6 is a limit cycle of $V = 16\mathrm{m/s}$, the amplitude of the limit cycle is $2A_{LC} = 0.8188$. Figure 7 is the amplitude response of A when $A_0 = 0.0001$, which means A is convergent when $A_0 < A_{LC}$ and the limit cycle is stable; Figure 8 is the amplitude response of A when $A_0 = 0.01$, which means A is divergent when $A_0 > A_{LC}$, while the limit cycle is stable. Figure 9 is the relationship of A and V, when $V \geq V_0$, the system is unstable. And when $V < V_0$, the system is stable and the amplitude of limit cycle is decreasing with V being bigger than V_0, and $G'(A_{LC}) = 0.0272$. Figure 10 is the relationship of limit cycle amplitude and velocity, the unstable area is increasing with increasing of freeplay. when $V < V_0$, the system is stable no matter the initial disturbance is bigger than limit cycle amplitude or not; when $V > V_0$, the system is unstable.

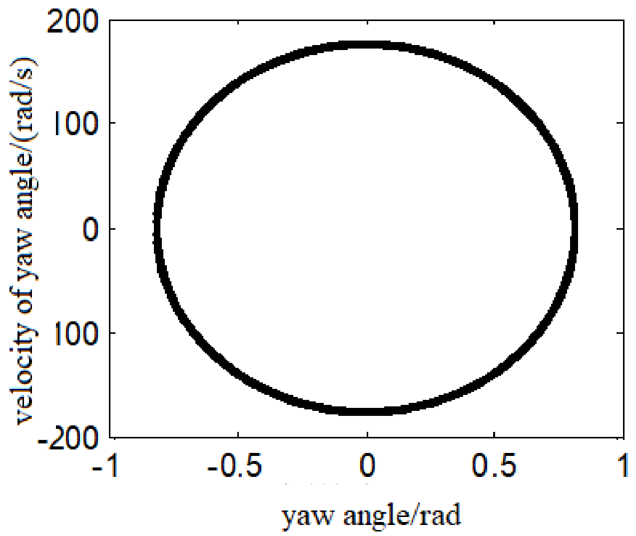

Fig.6 Limit cycle for only Coulomb ($C_{cf} = 0N.m, \theta_{fp} = 0.001$)

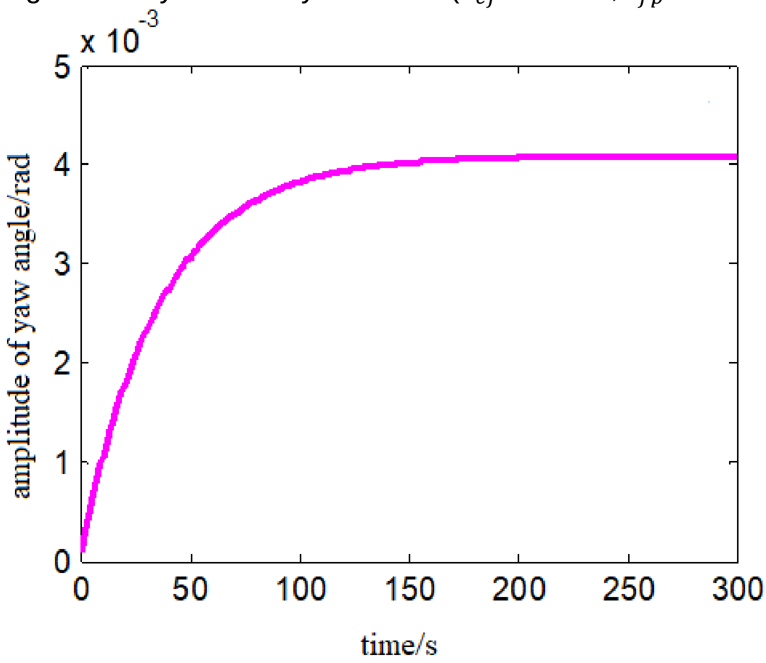

Fig.7 Response of yaw angle for only Coulomb ($C_{cf} = 0N.m, \theta_{fp} = 0.001, A_0 = 0.0001rad$)

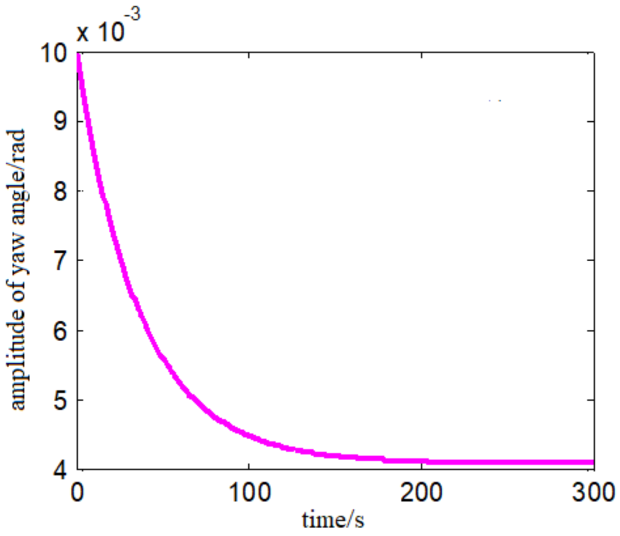

Fig.8 Response of yaw angle for only Coulomb ($C_{cf} = 0N.m, \theta_{fp} = 0.001, A_0 = 0.01rad$)

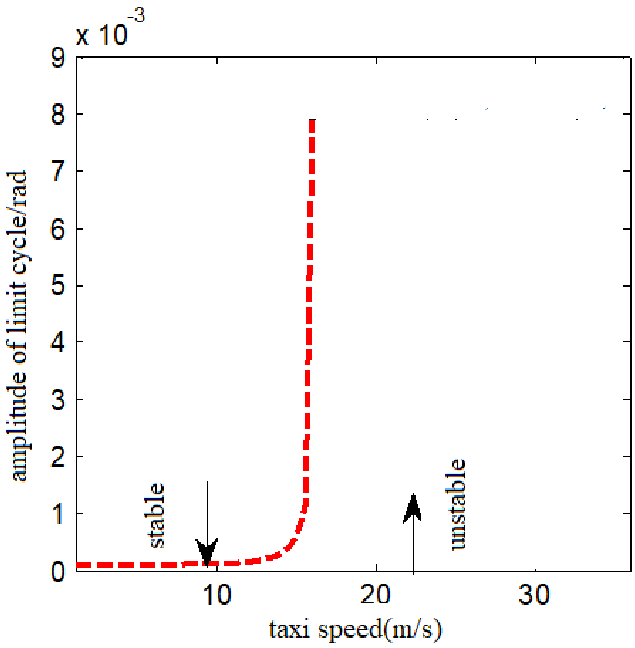

Fig.9 Limit Cycle Amplitude vs Taxi Speed ($C_{cf} = 0N.m, \theta_{fp} = 0.001$)

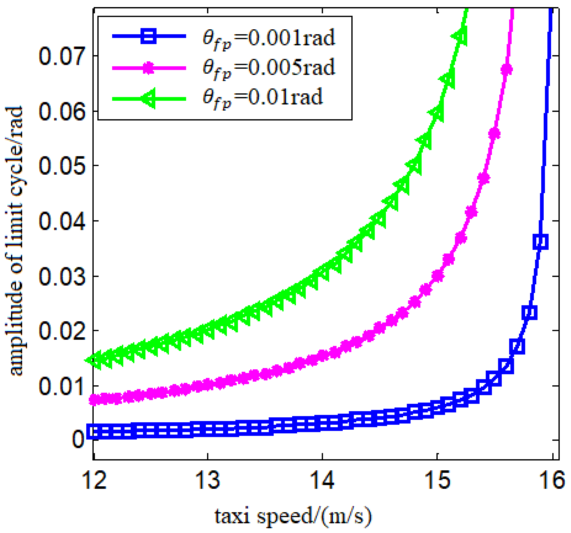

Fig.10 Limit Cycle Amplitude for different freeplay vs Taxi Speed

3.4 Freeplay and Coulomb Friction

Normalize $\boldsymbol{u}$ and make $\theta = q_{20} = 2A\sin\psi$, left eigenvector and right eigenvector can be obtained by equation (19) and equation (33).

$$\boldsymbol{u} = \begin{bmatrix} \omega_0 \\ -i \\ \dfrac{-i(\omega_0{}^2 t - i\omega_0 t V_0\beta - \beta V_0{}^2)}{V_0{}^2\alpha - \omega_0{}^2 + i\omega_0 V_0\beta} \\ \dfrac{-i(\omega_0{}^2 - i\omega_0 t V_0\alpha - \alpha V_0{}^2)}{V_0{}^2\alpha - \omega_0{}^2 + i\omega_0 V_0\beta} \end{bmatrix} = \begin{bmatrix} 215.5686 \\ -i \\ 0.0522 + 0.0765i \\ -0.0463 + 0.3169i \end{bmatrix} \tag{62}$$

$$\boldsymbol{v} = \begin{bmatrix} 1 \\ \dfrac{at(i\omega_0 + V_0\beta) + V_0\alpha b}{V_0{}^2\alpha - \omega_0{}^2 + i\omega_0 V_0\beta} \\ \dfrac{i\omega_0 b - atV_0}{V_0{}^2\alpha - \omega_0{}^2 + i\omega_0 V_0\beta} \\ i\dfrac{1}{2}\omega_0 I_z \end{bmatrix} = \begin{bmatrix} 1 \\ 59.5706 - 267.9573i \\ 5.2804 + 5.5801i \\ 343.1796i \end{bmatrix} \tag{63}$$

$\boldsymbol{f}_y^{(+1)}$ and $\boldsymbol{f}_y^{(+1)}$ can be got by equation (23) and equation (24) using piecewise integration.

$$\boldsymbol{f}_y^{(+1)} = \begin{bmatrix} -3.1831 \\ 0 \\ 0 \\ 0 \end{bmatrix} \tag{64}$$

$$\boldsymbol{f}_k^{(+1)} = \begin{bmatrix} -1.9099 \\ 0 \\ 0 \\ 0 \end{bmatrix} \tag{65}$$

σ, μ and γ can be obtained by equation (29), equation (30) and equation (31) respectively for every single velocity.

For a fleet aircraft, considering both freeplay and Coulomb friction, the analysis result is same as the result of considering freeplay only, which is relevant to the system parameters. For $V < V_0$, the system is stable, no matter the initial disturbance is bigger than limit cycle amplitude or not. For $V > V_0$, the system is unstable. Figure 11 is the relationship of limit cycle amplitude and velocity, the amplitude of limit cycle is decreasing far away from critical velocity。

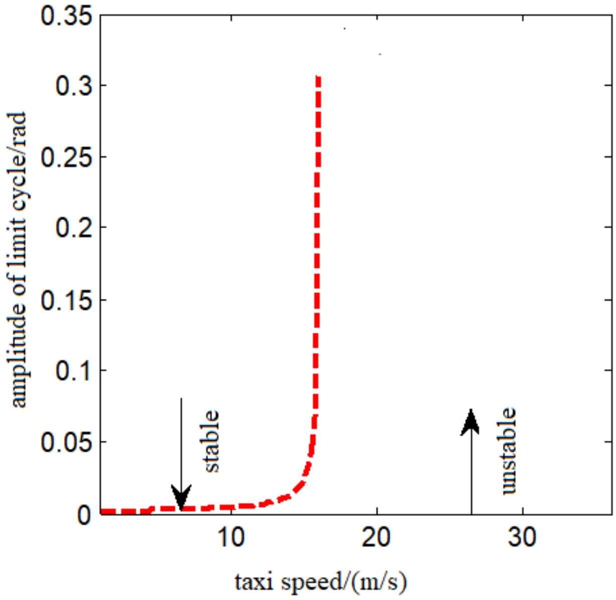

Fig.11 Limit Cycle Amplitude vs Taxi Speed ($C_{cf} = 5N.m, \theta_{fp} = 0.001$)

4. Conclusion

（1）For the fleet aircraft, Only Coulomb considered, the system is stable under the critical velocity. When above the critical velocity, the system is unstable if the disturbance is greater than limit cycle amplitude and the unstable zone is decreasing with increasing of Coulomb friction. Only freeplay considered, there is stable limit cycle under the critical velocity and unstable limit cycle above the critical velocity, the unstable zone is increasing with the increasing of freeplay. Both Coulomb and freeplay considered, the result is same with that of only considering freeplay in this case and it is related with the system parameters.

（2）The shimmy damping based on linear analysis is not always valid for pretending shimmy. From the perturbation analysis, the wheel stability is still related to the disturbance value, therefore, it is useful to decrease the disturbance when landing and to detect the landing gear freeplay in case of diverging quickly of yaw angle.

（3）For the fleet aircraft, it should decrease aircraft speed below the critical velocity if shimmy occurs when landing on the land; and it should raise the arresting ratio to suppress the shimmy of the fleet aircraft when landing on the deck, it can decrease unstable zone by increasing the torsion stiffness of the nose landing gear.

References

[1] ZHU D P. The theory of shimmy[M]. Beijing: National Defense Industry Press, 1984:20-24(in Chinese).

[2] ARREAZA C, BEHDINAN K, ZU J W. Linear stability analysis and dynamic response of shimmy dampers for main landing gears[J]. Journal of Applied Mechanics, 2016,83(3):63-72.

[3] NYBAKKEN G H. Investigation of tire parameter variations in wheel shimmy. Ph.D. Dissertation, University of Michigan, Dept. of Applied Mechanics, 1973.

[4] WU Z Z, GAO Z. Mechanical design[M]. Beijing: High Education Press, 2009: 119-140 (in Chinese).

[5] PACEJAK H B. The wheel shimmy phenomenon[D].Delft Technical Institute, Holland,1966.

[6] KRYLOV N M, BOGOLIUBOV N N. Introduction to nonlinear mechanics. Translated by LEFSCHETZ S, Princeton University Press, Princeton, N.J., Academy of Science, Ukraine S.S.R(1937), 1947.

[7] COLLINS R L. Theories on the mechanics of tires and their applications to shimmy analysis. Journal of Aircraft, 1971, 8(4):271-277.

[8] BURTON T D. Describing function analysis of nonlinear nose gear shimmy. In AS ME Paper 81-WA/DSC-20, 1981. Proceedings ASME Winter Annual Meeting Washington, D.C.

[9] SOMIESKI G. Shimmy analysis of a simple aircraft nose landing gear model using different mathematical methods. Aerospace Science and Technology, 1997,(8):545-555.

[10] WANG XUEJUN. The stability analysis of nose wheel shimmy.[D].Nanjing: Nanjing University of Aeronautics and Astronautics,2000. (in Chinese).

[11] LI SHEN. Study on mechanism and control strategies of vehicle steering wheel shimmy with bifurcation theories.[D].Jilin: Jilin University, 2005. (in Chinese).

[12] STEPAN G. Appell-gibbs equation for classical wheel shimmy - an energy view, Journal of Computational and Applied Mechanics, 2002,3(1): 85–92.

[13] TAKACS D, STEPAN G, HOGANS. J. Isolated large amplitude periodic motions of towed rigid wheels. Nonlinear Dynamics, 2008, 52(1-2): 27–34.

[14] COETZEE E, KRAUSKOPF B, LOWENBERG M H. Nonlinear analysis of aircraft ground handling, Proceedings of ICGF 2006, 2006.

[15] THOTA P, KRAUSKOPF B, LOWENBERG M. Bifurcation analysis of nose-landing-gear shimmy with lateral and longitudinal bending. Journal of Aircraft, 2010, 47(1): 87–95.

[16] KUO C C, L MORINO, DUGUNDJI. Perturbation and harmonic balance methods for nonlinear panel flutter. AIAA,1972, 10(11):1479-1484.

[17] GORDON J T, MERCHANT H C. An asymptotic method for predicting amplitudes of nonlinear wheel shimmy. Journal of Aircraft,1978, 15(3):155-159.

[18] GORDON J T. A perturbation Analysis of Nonlinear WheelShimmy.42nd IAA/ASME/ASCE/AHS/ACS Structure, Structure Dynamics, and Material conference, April 2001:1-18.

[19] NAYFEH A H, MOOK D T. Nonlinear Oscillations. John Wiley & Sons, Inc., New York, New York, first edition, 1979.

[20] HUANG L, HOLLOT C V. Results on positive pairs of polynomials and their application to the construction of stability domains, Inter J of Contro1,1987, 46(1).

[21] GJB 5097-2002. Design requirements of anti-shimmy for nose landing gear of aircraft[S]. 2003(in Chinese).

Copyright Statement